0022-3565/09/3311-45–53$20.00
THE JOURNAL OF PHARMACOLOGY AND EXPERIMENTAL THERAPEUTICS
JPET 331:45–53, 2009

Vol. 331, No. 1
155630/3513262
*Printed in U.S.A.*

# Structure-Activity Relationship Studies of Fostriecin, Cytostatin, and Key Analogs, with PP1, PP2A, PP5, and ($\beta$12–$\beta$13)-Chimeras (PP1/PP2A and PP5/PP2A), Provide Further Insight into the Inhibitory Actions of Fostriecin Family Inhibitors

Mark R. Swingle, Lauren Amable, Brian G. Lawhorn, Suzanne B. Buck, Christopher P. Burke, Pukar Ratti, Kimberly L. Fischer, Dale L. Boger, and Richard E. Honkanen

*Department of Biochemistry and Molecular Biology, University of South Alabama College of Medicine, Mobile, Alabama (M.R.S., L.A., P.R., K.L.F., R.E.H.); and Department of Chemistry and the Skaggs Institute for Chemical Biology, the Scripps Research Institute, La Jolla, California (B.G.L., S.B.B., C.P.B., D.L.B.)*

Received April 28, 2009; accepted July 8, 2009

**ABSTRACT**

Fostriecin and cytostatin are structurally related natural inhibitors of serine/threonine phosphatases, with promising antitumor activity. The total synthesis of these antitumor agents has enabled the production of structural analogs, which are useful to explore the biological significance of features contained in the parent compounds. Here, the inhibitory activity of fostriecin, cytostatin, and 10 key structural analogs were tested in side-by-side phosphatase assays to further characterize their inhibitory activity against PP1c (Ser/Thr protein phosphatase 1 catalytic subunit), PP2Ac (Ser/Thr protein phosphatase 2A catalytic subunit), PP5c (Ser/Thr protein phosphatase 5 catalytic subunit), and chimeras of PP1 (Ser/Thr protein phosphatase 1) and PP5 (Ser/Thr protein phosphatase 5), in which key residues predicted for inhibitor contact with PP2A (Ser/Thr protein phosphatase 2A) were introduced into PP1 and PP5 using site-directed mutagenesis. The data confirm the importance of the C9-phosphate and C11-alcohol for general inhibition and further demonstrate the importance of a predicted C3 interaction with a unique cysteine ($Cys^{269}$) in the $\beta$12–$\beta$13 loop of PP2A. The data also indicate that additional features beyond the unsaturated lactone contribute to inhibitory potency and selectivity. Notably, a derivative of fostriecin lacking the entire lactone subunit demonstrated marked potency and selectivity for PP2A, while having substantially reduced and similar activity against PP1 and PP1/PP2A- PP5/PP2A-chimeras that have greatly increased sensitivity to both fostriecin and cytostatin. This suggests that other features [e.g., the (*Z,Z,E*)-triene] also contribute to inhibitory selectivity. When considered together with previous data, these studies suggest that, despite the high structural conservation of the catalytic site in PP1, PP2A and PP5, the development of highly selective catalytic inhibitors should be feasible.

Fostriecin and cytostatin are structurally related phosphate monoesters produced by *Streptomyces pulveraceus* and *Streptomyces* sp. MJ654-Nf4, respectively, that display cytotoxicity and antitumor activity (for review, see Lewy et al., 2002). Cytostatin has cytotoxic activity toward melanoma and leukemia cell lines and has been shown to inhibit lung tumor metastasis (Masuda et al., 1995; Kawada et al., 1999). The antitumor activity of fostriecin (also called CI-920, NSC 339638, or PD 110,161) has been evaluated extensively (for review, see de Jong et al., 1997; Lewy et al., 2002; Honkanen, 2005). It demonstrates marked cytotoxicity against many cancer cell lines and potent antitumor activity in animals (for

This work was supported in part by the National Institutes of Health [Grants CA42056, CA60750, MD002314]. This investigation was conducted in a facility constructed with support from Research Facilities Improvement Program [Grant C06-RR11174] from the National Center for Research Resources.

M.R.S. and L.A. contributed equally to this work.

Article, publication date, and citation information can be found at http://jpet.aspetjournals.org.
doi:10.1124/jpet.109.155630.

**ABBREVIATIONS:** PP2A, Ser/Thr protein phosphatase 2A; PP2Ac, Ser/Thr protein phosphatase 2A catalytic subunit; PP1, Ser/Thr protein phosphatase 1; PP1c, Ser/Thr protein phosphatase 1 catalytic subunit; PP5c, Ser/Thr protein phosphatase 5 catalytic subunit; PPase, Ser/Thr phosphatase; SAR, structure-activity relationship; PAGE, polyacrylamide gel electrophoresis; PKA, protein kinase A; PIPES, 1,4-piperazinediethanesulfonic acid.

review, see de Jong et al., 1997; Lewy et al., 2002; Honkanen, 2005). To evaluate its potential for use as an antitumor agent in humans, fostriecin entered National Cancer Institute-sponsored clinical trials (Lê et al., 2004). Although limited, the data obtained from the phase 1 trials suggest that plasma levels of fostriecin shown to have antitumor activity in animals can be achieved in humans (Leopold et al., 1984; Susick et al., 1990; Lê et al., 2004). Unfortunately, the trials were discontinued before the maximal tolerated dose was established when concerns related to the storage stability of the naturally produced material surfaced (Lê et al., 2004).

The biological actions of fostriecin were initially ascribed to its ability to inhibit topoisomerase II; however, its cell-cycle effects and potency are inconsistent with this target of action (for review, see Lewy et al., 2002; Honkanen, 2005). Subsequently, fostriecin (Walsh et al., 1997; Buck et al., 2003), cytostatin (Bialy and Waldmann, 2004; Lawhorn et al., 2006), and structurally related natural products [phospholine, leustroducsin, and phoslactomycins (Usui et al., 1999; Kawada et al., 2003); Fig. 1] have all been shown to inhibit a subset of PPP-family serine/threonine protein phosphatases. Fostriecin acts as a potent inhibitor of PP2A/PP4 ($IC_{50}$ 0.2–4 nM) and a weak inhibitor of PP1 and PP5 (PP2A/PP4 versus PP1/PP5 selectivity $>10^4$) (Walsh et al., 1997; Buck et al., 2003). Cytostatin is also a potent and selective inhibitor of PP2A (PP2A $IC_{50}$ = 20–400 nM; PP2A versus PP1/PP5 > $10^3$) (Bialy and Waldmann, 2004; Lawhorn et al., 2006). Phospholine, leustroducsin H, and phoslactomycins are weaker inhibitors of PP2A (Usui et al., 1999; Kawada et al., 2003) and have not been examined using other phosphatases.

Synthetic efforts have provided methods for producing fostriecin and related PP2A-inhibitors. Following the first total synthesis of fostriecin (Boger et al., 2001), at least nine total or formal syntheses have been reported (Chavez and Jacobsen, 2001; Esumi et al., 2002; Reddy and Falck, 2002; Miyashita et al., 2003; Maki et al., 2005; Trost et al., 2005). The total synthesis of cytostatin (Bialy and Waldmann, 2004; Lawhorn et al., 2006; Jung et al., 2008) and cytostatin analogs (Lawhorn et al., 2006; Jung et al., 2008) have also been reported. These studies have sparked renewed interest in the potential for development of more stable derivatives that may have utility as novel antitumor drugs.

In efforts to identify the features of fostriecin-family compounds required for its potent and selective inhibition of PP2A, we have reported the synthesis of structural derivatives of fostriecin (Buck et al., 2003; Lawhorn et al., 2006) and, more recently, cytostatin (Lawhorn et al., 2006) that share distinctive phosphate monoester, (*Z,Z,E*)-triene, and α,β-unsaturated δ-lactone structural units (Fig. 1). Key analogs that have been synthesized include dephosphofostriecin, dephosphocytostatin, the C10/C11-diastereomers of cytostatin, a cyclic phosphodiester of fostriecin, a partial structure of fostriecin lacking the entire lactone moiety, and derivatives of fostriecin from which the lactone ring is saturated or contained in other modifications that alter the electrophilic nature of C3 (Buck et al., 2003; Lawhorn et al., 2006). The diastereomers of cytostatin demonstrated the importance of the C11-hydroxyl for PP2A inhibition (Lawhorn et al., 2006). Compounds in which the lactone is modified suggest that the lactone contributes to potent inhibitory activity against PP2A (Buck et al., 2003; Lawhorn et al., 2006). Compounds lacking the phosphate were less active against PP2A and less cytotoxic against cultured cancer cell lines (Buck et al., 2003; Lawhorn et al., 2006).

The crystal structures of PP1 (Goldberg et al., 1995), PP2A (Xing et al., 2006; Cho and Xu, 2007), and PP5 (Swingle et al., 2004) have been solved. Superpositions of PP1c, PP2Ac, and PP5c (Swingle et al., 2004) gives pairwise α-carbon root mean square deviations of 1.3 to 1.5 Å within the ~285-residue aligned region. This indicates that the similarity between the catalytic domains of PP1, PP2A, and PP5 is striking. Notably, the active site of all three PPases is located at the base of a shallow depression on the surface that is formed by the interstrand loops of a common central β-sandwich. When inhibition studies with fostriecin (Buck et al., 2003) and cytostatin (Lawhorn et al., 2006) are considered along with structural studies of PP2A (Buck et al., 2003; Xing et al., 2006), we predicted that the unsaturated lactone reacts with a cysteine near the active site of PP2A (Buck et al., 2003) and a hydrogen bond occurs between the C11-hydroxyl and $Arg^{214}$, which is a conserved binding feature of the nonselective PP1 pharmacophore (Colby and Chamberlin, 2006). The comparison of PP1, PP2A, and PP5 still reveals sequence and conformational differences near the active site, suggesting the feasibility of developing type-specific inhibitors. Notably, differences occur in the β12–β13 loop, a region immediately adjacent to the active site and known to participate in okadaic acid and microcystin-mediated inhibition of PP1 (Goldberg et al., 1995) and PP2A (Xing et al., 2006). Here, we performed site-directed mutagenesis of PP1c and PP5c, altering domains predicted to be important for inhibitor binding in PP2Ac. Head-to-head dose-response studies then were conducted with PP1c, PP2Ac, PP5c, and chimeras (PP1/PP2A and PP5/PP2A), testing key compounds for inhibitory activity.

## Materials and Methods

**Synthesis and Characterization of Inhibitors.** The synthesis and structural characterization of fostriecin, cytostatin, and structural analogs (compounds **1**, **2**, and **6-15**) has been described previously (Boger et al., 2001; Buck et al., 2003; Lawhorn et al., 2006).

**Preparation of Phosphohistone Substrate and Determination of Phosphatase Activity.** Phosphohistone, with a specific activity of $>4.5 \times 10^6$ dpm/nmol of incorporated phosphate, was prepared by the phosphorylation of bovine brain histone with cAMP-dependent protein kinase (PKA) from rabbit muscle in the presence of [$^{32}$P]ATP. Histone (type-2AS) was phosphorylated with PKA in a reaction containing 10 mg/ml histone, 2 mg/ml PKA, 6 mCi/ml [$\gamma$-$^{32}$P]ATP (200 mM ATP), 0.4 mM cAMP, 40 mM PIPES, pH 6.8 (at 37°C), 7 mM $MgCl_2$, 0.1 mM EDTA, and 5 mM dithiothreitol as described previously (Honkanen et al., 1990; Walsh et al., 1997; Swingle et al., 2007).

Protein phosphatase activity against phosphohistone was measured by the quantification of [$^{32}$P] liberated from phosphohistone, using established protocols (Honkanen et al., 1990; Swingle et al., 2007). In brief, dephosphorylation reactions were conducted for 10 min at 30°C. For all reactions, the dephosphorylation of substrate was kept to less than 10% of the total phosphorylated substrate, and the reactions were linear with respect to enzyme concentration and time. For inhibition studies, compounds were added to the enzymes 10 min before the initiation of the reaction by the addition of substrate. In the literature, the reported strength of PP2A inhibition for fostriecin and cytostatin varies considerably (e.g., $IC_{50}$ values range from 0.2 to 40 nM for fostriecin). This probably reflects differences in the amount of enzyme used in the assay, the choice of substrate,

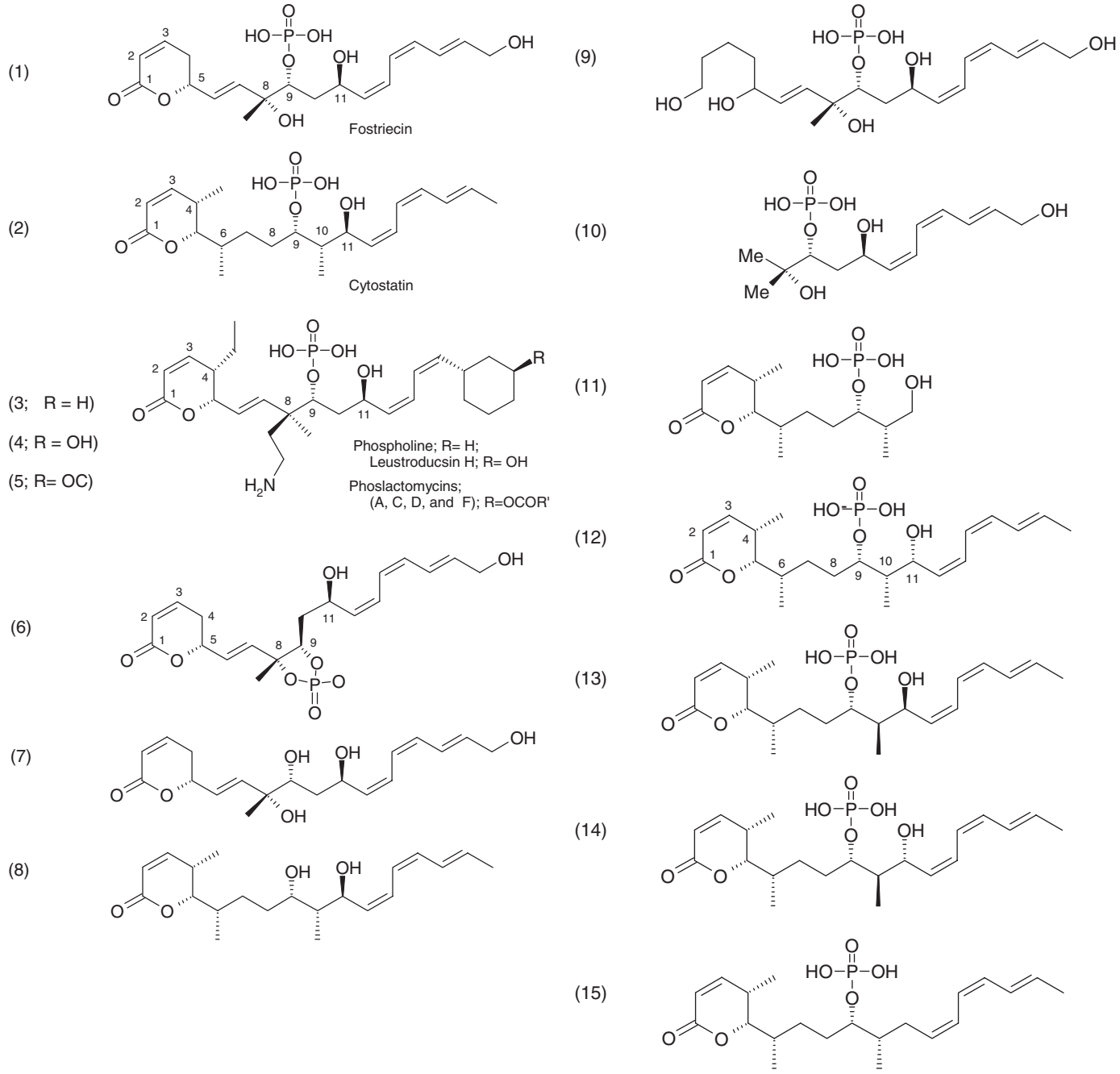


**Fig. 1.** Fostriecin family of inhibitors and structural derivatives. **1**, fostriecin. **2**, cytostatin. **3**, phospholine, R = H. **4**, leustroducsin H, R = OH. **5**, phoslactomycins (A, C, C, and F), R = OCOR′. **6**, (1*E*,3*R*,4*R*,6*R*,7*Z*,9*Z*,11*E*)-1-[(6*R*)-2-oxo-5,6-dihydro-2*H*-pyran-6-yl]-3,4,6,13-tetrahydroxy-3-*methyl*-1,7,9,11-tridecatetraene 3,4-cyclophosphate (fostriecin with C8–C9 cyclic phosphodiester). **7**, dephosphofostriecin. **8**, dephosphocytostatin. **9**, (5*R*,6*E*,8*R*,9*R*,11*R*,12*Z*,14*Z*,16*E*)-1,5,8,11,18-pentahydroxy-8-methyloctadeca-6,12,14,16-tetraen-9-yl dihydrogen phosphate (an electrophilic double bond reduction to provide a neutral alcohol). **10**, (2*E*,4*Z*,6*Z*,8*R*,10*R*)-11-*methyl*-2,4,6-dodecatriene-1,8,10,11-tetraol-10-phosphate (lactone ring deleted). **11**, cytostatin C1–C11 [cytostatin lacking the entire (*Z,Z,E*)-triene]. **12**, epi-(11*R*)-cytostatin. **13**, epi-(10*R*)-cytostatin. **14**, epi-(10*R*)-epi-(11*R*)-cytostatin. **15**, 11-deshydroxycytostatin (for details related to synthesis and nomenclature, see Buck et al., 2003; Lawhorn et al., 2006).

and/or handling/stability issues that are not widely appreciated [e.g., the inhibitory activity of fostriecin can be greatly reduced by even a brief exposure to weak acid (pH <5.5) or base pH >7.5 (Swingle et al., 2007)]. Therefore, when comparing the inhibitory actions of an analog series, it is important to consider stability issues and conduct side-by-side measurements using similar amounts of protein with the same substrate. All of the phosphatases employed were highly purified, demonstrating a single band upon SDS-PAGE and Coomassie Blue staining. For studies employing high affinity inhibitors, it is also important to ensure that the free inhibitor concentration in the assay is not reduced significantly through binding and sequestration of inhibitors by the PPase in the assay (i.e., "titration"). Here, a microcystin-titration assay (described in detail previously in Swingle et al., 2007) was used to accurately determine the amount of PPase used in the assays.

**Mutagenesis, Cloning, Expression, and Purification of PP1 and PP5.** Regions within the β12–β13 loop of human PP1c-α and PP5c were mutated at the residues indicated, replacing the amino acids endogenous to PP1 or PP5 with the corresponding residues contained in PP2Ac ($^{267}$YRCG$^{270}$ and combinations thereof) using

the QuikChange site-directed mutagenesis kit (Stratagene, La Jolla, CA). All resulting products were sequenced to verify the fidelity of the mutations and the integrity of the expression constructs. For expression, PP1c, PP5c, and the mutants produced (PP1-YRCG, PP5-YRCG) were cloned into a modified pMal-c2E expression vector (Swingle et al., 2004). Protein expression was induced with the addition of isopropyl β-D-thiogalactoside during logarithmic growth ($OD_{600}$ = 0.5). Cells were harvested by centrifugation at 6000*g* for 20 min at 4°C. The bacteria were resuspended in buffer A (20 mM Tris, pH 7.4, 10 μM EDTA, 0.001% Brij-35, 1 mM $MnCl_2$, 0.007% β-mercaptoethanol, and 20% glycerol) and lysed using a French press, followed by centrifugation at 45,000*g* for 1 h at 4°C. The proteins were purified using a nickel-iminodiacetate column as described previously (Swingle et al., 2004). The purified fusion proteins were then digested with TEV (Tobacco Etch Virus) protease, and free PP5c was further purified via anion-exchange chromatography using Q-Sepharose resin for PP5 as described previously (Swingle et al., 2004). Further purification of PP1 was achieved using a 5-ml HiTrap heparin column (GE Healthcare, Chalfont St. Giles, Buckinghamshire, UK) equilibrated with buffer A. PP1c was eluted using a 1 to 100% linear gradient of buffer B (20 mM Tris pH 7.4, 10 μM EDTA, 0.001% Brij-35, 1 mM $MnCl_2$, 0.007% β-mercaptoethanol, 20% glycerol, and 1 M NaCl). Changes made to the β12–β13 loop did not significantly affect column retention. Active fractions were identified by activity against *p*-nitrophenylphosphate (Sigma-Aldrich, St. Louis, MO). Fractions containing the highest *p*-nitrophenylphosphate phosphatase activity were pooled and stored at −80°C. The final preparations were >90% pure as judged by SDS-PAGE. Native PP2Ac was purified as described previously (Walsh et al., 1997).

**Computer Modeling of PP1, PP2A, PP5, and Inhibitors.** For inhibitor docking studies, AutoDock 3.05 (Morris et al., 1998) was modified to use a particle swarm optimization algorithm (Kennedy and Eberhart, 1995) as the search algorithm according to methods of Chen et al. (2007). Coordinate files for fostriecin were generated with a ghemical software program (Hassinen and Peräkylä, 2001). ADT (http://autodock.scripps.edu/ resources/adt/index_html) was used as a graphical user interface to the programs in the AutoDock suite (i.e., autotors, addsol, atmtobnd, protonate, autogrid3, autodock3, and makelaunch) and for analysis of docking results.

Atomic coordinates for the protein phosphatase 2A catalytic subunit (Xing et al., 2006) were obtained from the Research Collaboratory for Structural Bioinformatics Protein Data Bank (Protein Data Bank code 2ie4). All water molecules and okadaic acid were removed, and polar hydrogen atoms were added. Kollman united atom template charges (Kollman et al., 1984) were assigned with ADT. The solvation parameters (Stouten et al., 1993) were calculated with addsol. The prepared PP2Ac structure was saved in the PDBQS format required by autogrid3 for calculating energy grid maps. A rather large grid (80 × 62 × 68 points with 0.375 Å spacing) was defined for the calculation of maps, which encompassed the dinuclear catalytic center of PP2Ac as well as the "hydrophobic" and "acidic" grooves on the protein's surface.

All atom models of fostriecin were built with ghemical and optimized with the Tripos 5.2 force field. Gasteiger charges (Gasteiger and Marsili, 1980) were assigned to all atoms. At the physiological pH, the ligand phosphoryl groups are likely to be predominantly dianionic. Thus, for purposes of docking, phosphoryl groups were built completely unprotonated. All nonpolar hydrogens were merged within the united atom approach with autotors, which was also used to define which bonds were treated as freely rotatable during the docking run. Ligands were saved in the PDBQ format required by AutoDock 3.05. In the united atom approach, bonds to terminal methyl groups are not freely rotatable. However, hydroxyl groups are treated as rotatable because the hydrogen is polar. Because of their partial double-bond character, bonds in the triene tail were set as nonrotatable. The modified version of AutoDock described above was used to evaluate and optimize ligand binding energies over the conformational search space using a particle swarm optimization/local search hybrid algorithm. Population size was set to 50, and the number of energy evaluations was set to 5 million.

## Results

**Inhibition of PP1, PP2A and PP5 Phosphatase Activity.** Fostriecin, cytostatin, and a series of 10 structural analogs were synthesized using previously published methods (Buck et al., 2003; Lawhorn et al., 2006). In side-by-side measurements using equal amounts of enzymes and [$^{32}$P]phosphohistone as substrate, both fostriecin (**1;** $IC_{50}$ = 1.4 ± 0.3 nM) and cytostatin (**2**; $IC_{50}$ = 29.0 ± 7.0 nM) potently inhibit the activity of PP2A (Fig. 2). In contrast, dephosphofostriecin (**7**) and dephosphocytostatin (**8**) have minimal inhibitory activity against PP2A ($IC_{50}$ >100 μM). Derivatives, in which the entire lactone (**10**) or the entire (*Z,Z,E*)-triene (**11**) are deleted, strongly inhibit PP2A ($IC_{50}$ = 0.1 ± 0.02 and 4.2 ± 0.3 μM, respectively), while having little effect ($IC_{50}$ ≥100 μM) on PP1 or PP5 (Fig. 2, C and D).

**Inhibition of PP1/PP2A- and PP5/PP2A-Chimeras by Fostriecin.** Structural studies (Goldberg et al., 1995; Swingle et al., 2004) and mutational analysis (Zhang et al., 1996) indicate that both PP1 and PP5 share a common catalytic mechanism with PP2A. Indeed PP1, PP2A, PP2B, and PP5 all contain a common catalytic pocket consisting of 10 conserved amino acids (Fig. 3). Computer models predicted that fostriecin binds to a unique region of PP2A contained in the β12–β13 loop, and mutational analysis of PP1 revealed considerable insight into the binding of natural inhibitors (Zhang et al., 1994, 1996). Therefore, we performed site-directed mutagenesis, replacing endogenous amino acids in the β12–β13 loop of PP1 and PP5, with the corresponding amino acids (YRCG) in PP2A. In side-by-side dose-response studies, we then tested the sensitivity of the PP1(YRCG)- and PP5(YRCG)-chimeras to fostriecin, cytostatin, and key analogs. In PP1, conversion to YRCG resulted in an ~600-fold increase in sensitivity to fostriecin (Fig. 4A; $IC_{50}$ = 0.09 ± 0.02 versus ~72 ± 11 μM). With PP5, an ~200-fold increase in sensitivity was produced by a similar (YRCG) mutation (Fig. 4B; $IC_{50}$ = 0.3 ± 0.08 versus 60.5 ± 0.6 μM). Mutation of a single residue in PP5 (PP5 Met to Cys) increased sensitivity to fostriecin by ~50-fold ($IC_{50}$ = 1.2 ± 0.5 μM). PP1(YRCG) and PP5(YRCG) were also sensitive to cytostatin ($IC_{50}$ = 17 ± 3.2 and 34 ± 6.1 μM, respectively), which has little effect on native PP1 or PP5 ($IC_{50}$ >100 μM). Compounds, in which the lactone ring is deleted or disrupted (**9** and **10**), demonstrated no detectable increase in inhibitory activity against PP1(YRCG) or PP5(YRCG). In contrast, compounds retaining the phosphate monoester and unsaturated lactone (i.e., **1**, **2**, and **11–15**) demonstrated increased potency against the chimeras (Table 1).

## Discussion

To date, >10 natural compounds have been identified that share a distinctive phosphate monoester and α,β-unsaturated δ-lactone structural units with fostriecin (Fig. 1). Fostriecin and cytostatin, which both act as potent inhibitors of PP2A (Walsh et al., 1997; Buck et al., 2003; Lawhorn et al., 2006) also share a (*Z,Z,E*)-triene. The total synthesis of fostriecin (**1**) (Boger et al., 2001; Chavez and Jacobsen, 2001), cytostatin (**2**) (Lawhorn et al., 2006), and, more recently,

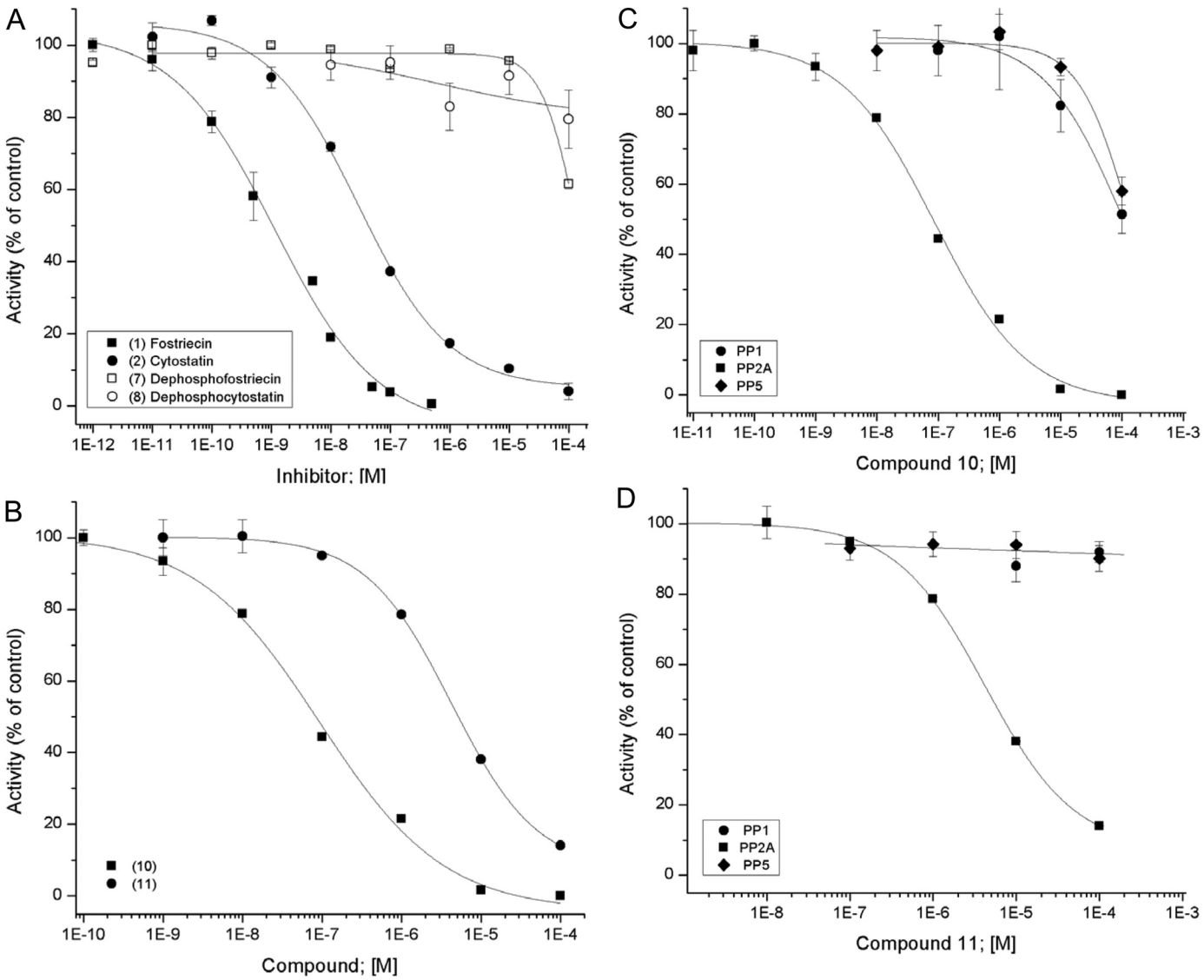


**Fig. 2.** Inhibitory effect of fostriecin family inhibitors and structural analogs on the activity of purified PPP-family phosphatases. A, effect of fostriecin (filled squares) (**1**), cytostatin (filled circles) (**2**), dephosphofostriecin (open squares) (**7**), and dephosphocytostatin (open circles) (**8**) on the activity of purified PP2Ac. B, effect of **10** (filled square) and **11** (filled circle) on the activity of PP2Ac. C, comparison of the inhibitory effect of **10** on the activity of PP2Ac (filled square), PP1 (filled circle), and PP5 (filled diamond). D, comparison of the inhibitory effect of **11** on the activity of PP2Ac (filled square), PP1 (filled circle), and PP5 (filled diamond). The structures and names of the inhibitors are provided in Fig. 1. Highly purified catalytic subunit of the indicated PPases were purified and assayed using [$^{32}$P]histone as a substrate as described under *Materials and Methods*. The data are expressed a percentage of controls, with control activity against phosphohistone for each PPase diluted to 750 ± 14 nmol/min/mg protein. All compounds were mixed with the enzymes for 10 min at 23°C before the initiation of the reaction with the addition of substrate. Each point represents the mean ± S.D. ($n$ = 8). $IC_{50}$ values are provided under *Results*.

several key analogs (**6–15**) (Buck et al., 2003; Lawhorn et al., 2006) have enabled further structure-activity relationship studies to explore the inhibitory activity of the fostriecin family of inhibitors. As known from previous studies (Buck et al., 2003; Lawhorn et al., 2006) and shown in Fig. 2A, fostriecin (**1;** $IC_{50}$ = 1.4 nM) is an ~20-fold more potent inhibitor of PP2A than cytostatin (**2**; $IC_{50}$ = 29.0 nM). At much higher concentrations, fostriecin is essentially an equipotent inhibitor of PP5 and PP1 ($IC_{50}$ ~60 μM), and cytostatin has little effect on PP1 or PP5 ($IC_{50}$ >100 μM). Thus, the selectivity of **1** and **2** for PP2A is substantial (PP2A/PP1-PP5 > $10^4$). The known (Buck et al., 2003; Lawhorn et al., 2006) importance of the C9 phosphate for both **1** and **2** is illustrated in Fig. 2A, where dephosphofostriecin (**7**) and dephosphocytostatin (**8**) have minimal inhibitory activity against PP2A ($IC_{50}$ >100 μM). When the phosphate is converted into a phosphodiester (**6**), inhibitory activity against PP2A is reduced ~$10^3$-fold ($IC_{50}$ 3.2 ± 1.1 μM). Both dephosphocompounds also have reduced inhibitory activity against PP1 and PP5 (data not shown), suggesting that the phosphate interacts with conserved catalytic residues. However, **1** and **2** also differ at C4 and C17. In addition, derivatives in which the entire lactone (**10**) or the entire (*Z,Z,E*)-triene (**11**) are deleted still strongly inhibit PP2A, while having little effect on PP1 or PP5 (Fig. 2, C and D). We interpret this to indicate that both the lactone and the (*Z,Z,E*)-triene contribute to selectivity.

Computer models of interactions between **1** or **2** with PPP-family phosphatases suggest that the phosphate and the common C11-hydroxyl interact with regions conserved in

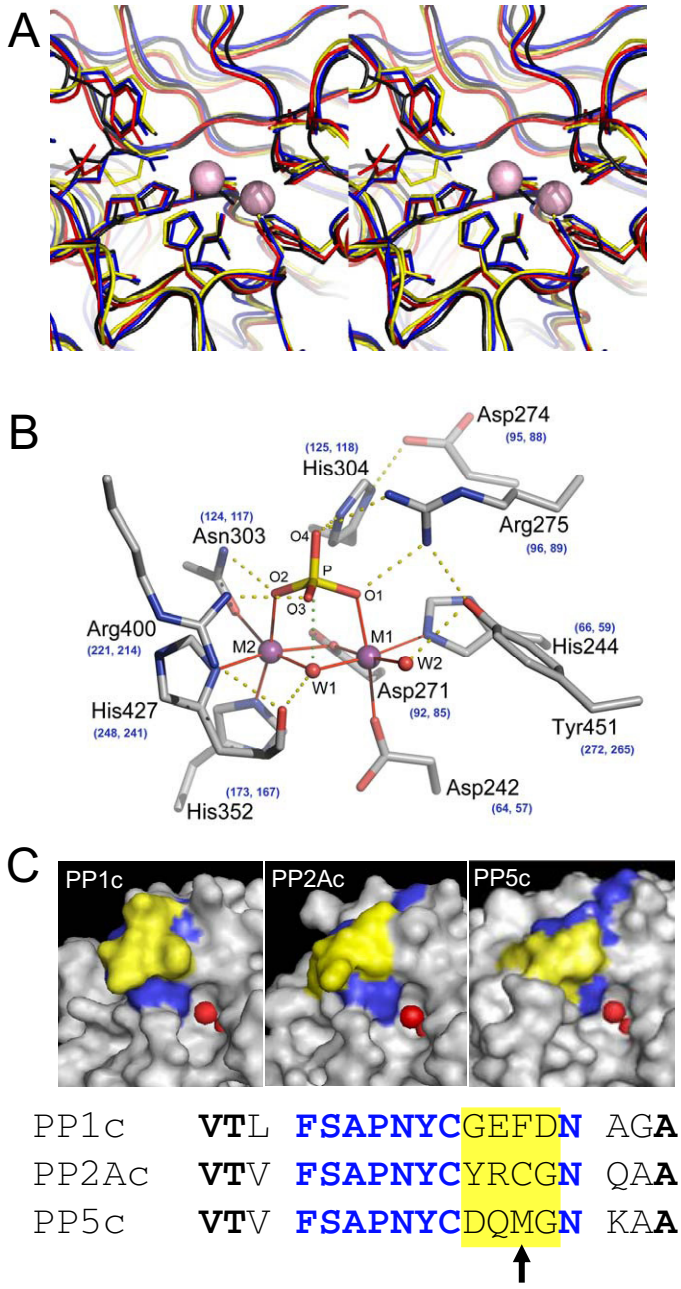


**Fig. 3.** Structural comparison of the catalytic pocket in PPP-family phosphatases. A, stereoview showing the superposition of the conserved active site residues. PP1, PP2A, PP2B, and PP5 share a common active motif consisting of $D^{64,57,242}XH^{66,59,244}(X)_{26-27}D^{92,85,271}XXD^{95,88,274}R^{96,89,275}(X)_{28}N^{124,117,303}H^{125,118,304}(X)_{48}H^{173,167,352}(X)_{48-54}R^{221,214,400}(X)_{27}H^{248,241,427}$, where X represents variable amino acids and the superscript numbers correspond to the primary amino acid sequence of PP1, PP2A, and PP5, respectively. PP1-α (red), PP5 (blue), PP2B (yellow), and PP2A (black) are from Protein Data Bank codes 1jk7, 1s95, 1tco, and 2ie4, respectively. Superpositions were performed with STRAP (http://www.charite.de/bioinf/strap/). B, detailed representation of key substrate contacts in the catalytic site shared by PP1, PP2A, and PP5. The active site residues were positioned using the data from the structure of PP5c (Protein Data Bank code 1s95), with PP1 and PP2A numbering shown in blue. Through hydrogen bonds (yellow dotted lines), four conserved amino acids ($Arg^{96,89,275}$, $Asn^{124,117,303}$, $His^{125,118,304}$, and $Arg^{221,214,400}$) help position the substrate for nucleophilic attack. The other six function as metal-coordinating residues (coordination bonds shown as red solid lines), which position and help activate a ligated hydroxide that acts as a nucleophile in the catalytic reaction (Swingle et al., 2004). These 10 amino acids are positioned by the compact α/β-fold composed of 11 α-helices and 14 β-strands common to PP1, PP2A, and PP5. The metal activated water is shown as a green sphere (W1) in a near nucleophilic-attack configuration of the substrate phosphate (P). C, surface-filled models illustrating the catalytic pocket and β12–β13 region of PP1c, PP2Ac, and PP5c. Surface-filled models of PP1c, PP2Ac, and PP5c were generated from the Protein Data Bank codes (as above) using PyMOL (http://www.pymol.org/). The amino acids comprising the β12–β13 loop are colored, with the variable amino acids affecting sensitivity to fostriecin shown in yellow and the conserved residues shown in blue. Catalytic metals are shown as red spheres. An alignment of the single letter codes for the primary amino acids contained in the β12–β13 loops for PP1, PP2A, and PP5 is shown below with the same color scheme.

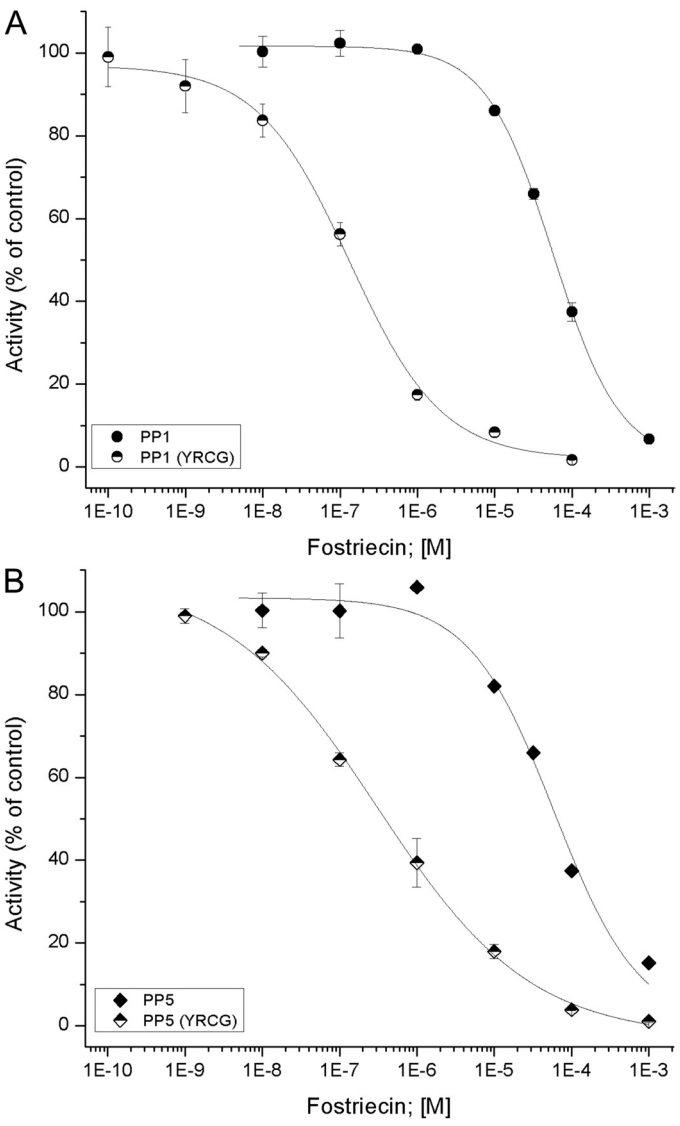


**Fig. 4.** Effect of mutations in the β12–β13 loop on the sensitivity of PP1 and PP5 to fostriecin. Site-directed mutagenesis was used to generate mutant constructs of PP1 and PP5, replacing the endogenous amino acids in PP1 and PP5 with the amino acids YRCG contained in β12–β13 loop of PP2A predicted to aid fostriecin binding by SAR and structural studies. Mutations were constructed and expressed in *E. coli* and purified to near homogeneity as determined by Coomassie Blue staining of SDS-PAGE gels. Inhibition assays were conducted as described above (Fig. 2). A, comparison of PP1 sensitivity to fostriecin, wild type (filled circle), and PP1/PP2A(YRCG)-chimera (half-filled circle). B, comparison of PP5 sensitivity to fostriecin, wild type (filled diamonds), and PP5/PP2A(YRCG)-chimera (half-filled diamonds).

PP1, PP2A, and PP5 (i.e., the catalytic metals and conserved active site residues that coordinate the metals and/or position the incoming substrate for nucleophilic attack), which is consistent with the inhibition data presented above. The

TABLE 1

Comparison of inhibitory activity

Phosphatase inhibition assays were conducted with native PP2Ac and recombinant human PP1c and PP5c expressed in *E. coli* as described previously (Honkanen et al., 1990; Walsh et al., 1997; Swingle et al., 2004, 2007). Assays were conducted side-by-side using similar amount of enzyme and [$^{32}$P]phosphohistone as a substrate. Native PP1 and PP5 (bovine brain) and the human recombinant proteins used here demonstrated similar activity (Swingle et al., 2004, 2007) and sensitivity to fostriecin, cytostatin, and other known inhibitors [i.e. okadaic acid, cantharidin, calyculin A, and microcystin-LR (Honkanen et al., 1990; Swingle et al., 2007)]. The data shown represent the mean ± S.D., $n > 5$.

| Compound | $IC_{50}$ Values | | | | |
|---|---|---|---|---|---|
| | PP2A | PP1 | PP1(YRCG) | PP5 | PP5(YRCG) |
| | | | $\mu M$ | | |
| Fostriecin | | | | | |
| **1** | 0.0014 ± 0.0003 | 72 ± 11 | 0.09 ± 0.02 | 60 ± 0.6 | 0.30 ± 0.08 |
| Cytostatin | | | | | |
| **2** | 0.029 ± 0.007 | >100 | 17 ± 3.2 | >100 | 34 ± 6.1 |
| **7** | >100 | >100 | >100 | >100 | >100 |
| **8** | >100 | >100 | >100 | >100 | >100 |
| **9** | 2.1 ± 0.6 | >100 | >100 | >100 | >100 |
| **10** | 0.1 ± 0.02 | ~100* | ~100* | >100 | >100 |
| **11** | 4.2 ± 0.3 | >100 | 11 ± 4.1 | >100 | 35 ± 3.9 |
| **12** | 19.0 ± 1.7 | >100 | 24 ± 1.3 | >100 | N.D. |
| **13** | 21 ± 1.6 | >100 | 20 ± 1.4 | >100 | 19 ± 4.3 |
| **14** | 3.8 ± 0.4 | 57 ± 6.8 | 10 ± 4.2 | >100 | N.D. |
| **15** | 6.9 ± 0.7 | >100 | 13 ± 1.9 | >100 | N.D. |

* Enzyme inhibition at 100 μM = 44 to 55%.

models also predict that the unsaturated lactone contributes to the strong inhibitory actions of PP2A due to an electrophilic interaction with a cysteine ($Cys^{269}$) contained in the β12–β13 loop of PP2A that is not present in PP1 and PP5 (Fig. 3C). This prediction is supported by the decreased PP2A inhibitory activity of **9**, in which the electrophilic nature of C3 is absent, and **10**, in which the entire lactone moiety is deleted (Fig. 2, C and D). To further test this hypothesis, we performed site-directed mutagenesis, replacing endogenous amino acids in the β12–β13 loop of PP1 and PP5, with the corresponding amino acids in PP2A. For both PP1 and PP5, the region needed for strong inhibition was mapped to four amino acids immediately adjacent to the active site tyrosine ($Tyr^{265}$). In PP1, conversion from GEFD to YRCG (the sequence contained in PP2A) resulted in an ~600-fold increase in sensitivity to fostriecin (Fig. 4A). With PP5, an ~200-fold increase in sensitivity was produced by a similar (DQMG to YRCG) mutation (Fig. 4B). PP1- and PP5-YRCG mutants were also sensitive to cytostatin ($IC_{50}$ = 17 ± 3.2 and 34 ± 6.1 μM, respectively), which has little effect on native PP1 or PP5 ($IC_{50}$ >100 μM). Compounds in which the lactone ring is deleted or disrupted (**9** and **10**) demonstrated no detectable increase in inhibitory activity against PP1(YRCG) or PP5(YRCG). In addition, **11**, which lacks the (*Z,Z,E*)-triene, demonstrated similar strength in the inhibition of PP2A, PP1(YRCG), and PP5(YRCG) while having minimal activity against native PP1 or PP5. Together, these studies support the critical role of an interaction between C3 and $Cys^{269}$ in the β12–β13 loop of PP2A. The critical role of $Cys^{269}$ in fostriecin sensitivity is also supported by our previous SAR studies using additional derivatives of fostriecin (Buck et al., 2003) and studies in yeast, in which a 10-fold decrease in sensitivity to fostriecin induced by random mutagenesis was associated with a homologous C269S mutation (Evans and Simon, 2001).

In addition to the lactone, **1**, **2**, and **11** share in common a C11-alcohol, and C10 of **2** and **11** contains a methyl group not contained in **1**, **9**, or **10**. Thus, four C10/C11-cytostatin diastereomers (**12**, **13**, **14**, and **15**) were tested on PP1, PP2A, and PP1(YRCG). As we reported previously (Buck et al., 2003; Lawhorn et al., 2006), compared to the natural compound (**2**), each of these cytostatin diastereomers was a less potent inhibitor of PP2A. The C11-epimer (**12**), in which only the stereochemistry of the alcohols is inverted, the C10-epimer (**13**), in which only the stereochemistry of the methyl group is inverted, and the (10*R*,11*R*)-diastereomer (**14**), in which both the C11-methyl group and the C11-alcohol are inverted, all proved to be stronger inhibitors of PP1(YRCG) than PP1 (Table 1). All three cytostatin epimers also demonstrated similar strength against PP1(YRCG) and PP2A. In addition, **15**, which lacks the alcohol at C11, and **11**, which lacks the entire triene, also demonstrated similar strength of inhibition against PP2A and PP1(YRCG) while having little effect on native PP1 or PP5. Together, these observations provide compelling data supporting the concept that much of the selectivity for PP2A observed with fostriecin-family inhibitors is indeed derived from the interaction between C3 of the inhibitors and the β12–β13 loop in PP2A. Nonetheless, because **9** and **10** are still highly selective for PP2A (Fig. 2), additional selectivity is likely derived from the (*Z,Z,E*)-triene.

To gain additional insight into the interactions that aid the selective inhibition of PP2A, bound conformations of **1** were generated via molecular docking with a modified version of AutoDock 3.05 (see *Materials and Methods*). Cluster analysis of top-scoring poses from each of 100 independent docking runs separated poses into nonoverlapping groups based upon a root mean square deviation threshold of 2.5 Å. Each cluster represents a group of similar binding poses, the degree of similarity being dependent upon the root mean square deviation cutoff. These clusters can be thought of as representing a binding mode plus snapshots of the associated relative internal motions of the receptor-ligand complex (Ruvinsky and Kozintsev, 2005).

The docking of fostriecin to PP2Ac results in 33 nonoverlapping clusters (eight with more than two members). The three clusters with the lowest estimated binding energy (ranked according to the best member) show fostriecin bound (for a representative structure; see Fig. 5) with the phosphate moiety coordinated to the active site metals and forming hydrogen bonds with highly conserved active site residues

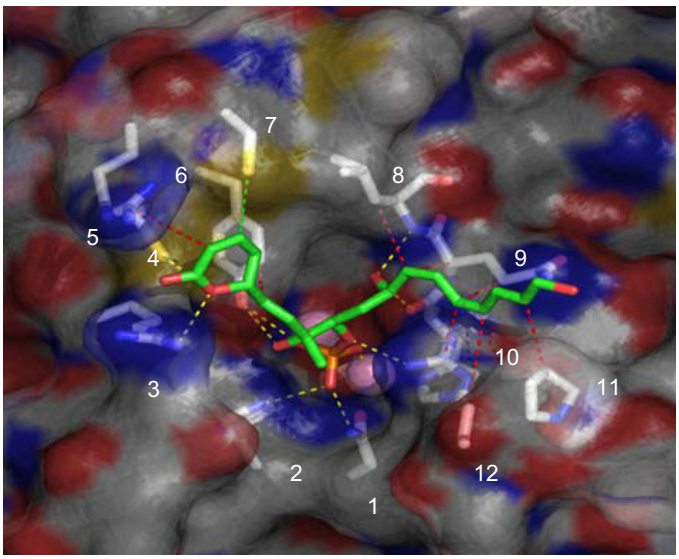


**Fig. 5.** Interactions of fostriecin with PP2A. AutoDock was used to obtain bound conformations of fostriecin. Representative docked conformation of fostriecin with the (*Z,Z,E*)-triene placed in the acidic groove (fostriecin = stick representation, PP2A = surface representation) and predicted interactions with PP2A (represented as dashed lines, yellow = hydrogen bonds, red = hydrophobic interactions, green = interaction with nucleophilic γ-sulfur of $Cys^{269}$). Interacting residues are shown as sticks beneath the partially transparent PP2A molecular surface: $Asn^{117}$, $His^{118}$, $Arg^{89}$, $Cys^{266}$, $Arg^{268}$, $Tyr^{265}$, $Cys^{269}$, $Leu^{243}$, $Gln^{242}$, $His^{241}$, $Pro^{213}$, and $Arg^{214}$ are labeled 1–12, respectively.

($Asn^{117}$, $His^{118}$, $Arg^{214}$, and $Tyr^{265}$), the (*Z,Z,E*)-triene placed in the acidic groove, and the unsaturated lactone ring nestled in a pocket formed by the highly conserved $Arg^{89}$ and four residues in the β12–β13 loop: $Tyr^{265}$, $Cys^{266}$, $Arg^{268}$, and $Cys^{269}$. It is important to note that this conformation places the γ-sulfur of $Cys^{269}$ 3.6 Å away from the electrophilic C3, suggesting that binding to PP2A prepositions the lactone ring for nucleophilic attack. Two of the residues in the lactone binding pocket, $Arg^{268}$ and $Cys^{269}$, are nonconservatively substituted in PP1 and PP5. $Arg^{268}$ is substituted by Glu and Gln in PP1 and PP5, respectively, whereas $Cys^{269}$ is substituted by Phe and Met. In addition to the absence of the thiolate nucleophile in $Cys^{269}$, the presence of the bulky hydrophobic side chain of Phe or Met in the other two PPases alters the shape of the pocket such that the lactone binding would be less favorable. The structure of PP5 also shows partial occupancy of this pocket by a methionine residue from the C-terminal J-helix that may interfere with binding. The C8-hydroxyl forms a hydrogen bond with the $Tyr^{265}$ hydroxyl group and would be well placed to form a hydrogen bond with the guanidinium group of $Arg^{89}$ if receptor flexibility allows for an induced fit of receptor residues around this fostriecin conformation. The C11-hydroxyl forms a hydrogen bond with the backbone amide of $Leu^{243}$ and the backbone carbonyl of the highly conserved $His^{241}$, which has been implicated in helping to orient the hydroxide nucleophile during phosphomonoester hydrolysis (Swingle et al., 2004). The triene tail makes hydrophobic contacts with the side chains of $Pro^{213}$ and $Leu^{243}$, as well as the aliphatic portion of $Gln^{242}$. These residues are not conserved with PP5 or, with the exception of $Gln^{242}$, PP1. These structural differences, with regard to interactions with the triene tail, may account for part of the differential affinity of fostriecin toward these enzymes. Unfortunately, unlike the β12–β13 loop, which is contained on an exposed surface loop and can easily be modified without affecting that general structure of PP1 and PP5, mutations of the residues in the acidic grove are likely to alter large regions of the protein. Therefore, future SAR studies await the development of methods to synthesize additional derivatives to further probe the importance of the triene.

## References


Bialy L and Waldmann H (2004) Total synthesis and biological evaluation of the protein phosphatase 2A inhibitor cytostatin and analogues. *Chemistry* **10:**2759–2780.

Boger DL, Ichikawa S, and Zhong W (2001) Total synthesis of fostriecin (CI-920). *J Am Chem Soc* **123:**4161–4167.

Buck SB, Hardouin C, Ichikawa S, Soenen DR, Gauss CM, Hwang I, Swingle MR, Bonness KM, Honkanen RE, and Boger DL (2003) Fundamental role of the fostriecin unsaturated lactone and implications for selective protein phosphatase inhibition. *J Am Chem Soc* **125:**15694–15695.

Chavez DE and Jacobsen EN (2001) Total synthesis of fostriecin (CI-920). *Angew Chem Int Ed Engl* **40:**3667–3670.

Chen HM, Liu BF, Huang HL, Hwang SF, and Ho SY (2007) SODOCK: swarm optimization for highly flexible protein-ligand docking. *J Comput Chem* **28:**612–623.

Cho US and Xu W (2007) Crystal structure of a protein phosphatase 2A heterotrimeric holoenzyme. *Nature* **445:**53–57.

Colby DA and Chamberlin AR (2006) Pharmacophore identification: the case of the Ser/Thr protein phosphatase inhibitors. *Mini Rev Med Chem* **6:**657–665.

de Jong RS, de Vries EG, and Mulder NH (1997) Fostriecin: a review of the preclinical data. *Anticancer Drugs* **8:**413–418.

Esumi T, Okamoto N, and Hatakeyama S (2002) Versatile enantiocontrolled synthesis of (+)-fostriecin. *Chem Commun (Camb)* **24:**3042–3043.

Evans DR and Simon JA (2001) The predicted beta12-beta13 loop is important for inhibition of PP2Acalpha by the antitumor drug fostriecin. *FEBS Lett* **498:**110–115.

Gasteiger J and Marsili M (1980) Iterative partial equalization of orbital electronegativity—a rapid access to atomic charges. *Tetrahedron* **36:**3219–3228.

Goldberg J, Huang HB, Kwon YG, Greengard P, Nairn AC, and Kuriyan J (1995) Three-dimensional structure of the catalytic subunit of protein serine/threonine phosphatase-1. *Nature* **376:**745–753.

Hassinen T and Peräkylä M (2001) New energy terms for reduced protein models implemented in an off-lattice force field. *J Comput Chem* **22:**1229–1242.

Honkanen RE (2005) Serine/threonine protein phosphatase inhibitors with antitumor activity. *Handbk Exp Pharm* **167:**295–317.

Honkanen RE, Zwiller J, Moore RE, Daily SL, Khatra BS, Dukelow M, and Boynton AL (1990) Characterization of microcystin-LR, a potent inhibitor of type 1 and type 2A protein phosphatases. *J Biol Chem* **265:**19401–19404.

Jung WH, Guyenne S, Riesco-Fagundo C, Mancuso J, Nakamura S, and Curran DP (2008) Confirmation of the stereostructure of (+)-cytostatin by fluorous mixture synthesis of four candidate stereoisomers. *Angew Chem Int Ed Engl* **47:**1130–1133.

Kawada M, Amemiya M, Ishizuka M, and Takeuchi T (1999) Differential induction of apoptosis in B16 melanoma and EL-4 lymphoma cells by cytostatin and bactobolin. *Jpn J Cancer Res* **90:**219–225.

Kawada M, Kawatsu M, Masuda T, Ohba S, Amemiya M, Kohama T, Ishizuka M, and Takeuchi T (2003) Specific inhibitors of protein phosphatase 2A inhibit tumor metastasis through augmentation of natural killer cells. *Int Immunopharmacol* **3:**179–188.

Kennedy J and Eberhart RC (1995) Particle swarm optimization, in *Proceedings of IEEE International Conference on Neural Networks*, (Perth, WA, Australia), Vol. 4, pp 1942–1948. IEEE Service Center, Piscataway, NJ.

Lawhorn BG, Boga SB, Wolkenberg SE, Colby DA, Gauss CM, Swingle MR, Amable L, Honkanen RE, and Boger DL (2006) Total synthesis and evaluation of cytostatin, its C10–C11 diastereomers, and additional key analogues: impact on PP2A inhibition. *J Am Chem Soc* **128:**16720–16732.

Lê LH, Erlichman C, Pillon L, Thiessen JJ, Day A, Wainman N, Eisenhauer EA, and Moore MJ (2004) Phase I and pharmacokinetic study of fostriecin given as an intravenous bolus daily for five consecutive days. *Invest New Drugs* **22:**159–167.

Leopold WR, Shillis JL, Mertus AE, Nelson JM, Roberts BJ, and Jackson RC (1984) Anticancer activity of the structurally novel antibiotic Cl-920 and its analogues. *Cancer Res* **44:**1928–1932.

Lewy DS, Gauss CM, Soenen DR, and Boger DL (2002) Fostriecin: chemistry and biology. *Curr Med Chem* **9:**2005–2032.

Maki K, Motoki R, Fujii K, Kanai M, Kobayashi T, Tamura S, and Shibasaki M (2005) Catalyst-controlled asymmetric synthesis of fostriecin and 8-epi-fostriecin. *J Am Chem Soc* **127:**17111–17117.

Masuda T, Watanabe S, Amemiya M, Ishizuka M, and Takeuchi T (1995) Inhibitory effect of cytostatin on spontaneous lung metastases of B16-BL6 melanoma cells. *J Antibiot (Tokyo)* **48:**528–529.

Miyashita K, Ikejiri M, Kawasaki H, Maemura S, and Imanishi T (2003) Total synthesis of an antitumor antibiotic, fostriecin (CI-920). *J Am Chem Soc* **125:**8238–8243.

Morris GM, Goodsell DS, Halliday RS, Huey R, Hart WE, Belew RK, and Olson AJ (1998) Automated docking using a Lamarckian genetic algorithm and an empirical binding free energy function. *J Comput Chem* **19:**1639–1662.

Reddy YK and Falck JR (2002) Asymmetric total synthesis of (+)-fostriecin. *Org Lett* **4:**969–971.

Ruvinsky AM and Kozintsev AV (2005) New and fast statistical-thermodynamic

method for computation of protein-ligand binding entropy substantially improves docking accuracy. *J Comput Chem* **26:**1089–1095.
Stouten PFW, Frömmel C, Nakamura H, and Sander C (1993) An effective solvation term based on atomic occupancies for use in protein simulations. *Mol Simulat* **10:**97–120.
Susick RL Jr, Hawkins KL, and Pegg DG (1990) Preclinical toxicological evaluation of fostriecin, a novel anticancer antibiotic, in rats. *Fundam Appl Toxicol* **15:**258–269.
Swingle M, Ni L, and Honkanen RE (2007) Small-molecule inhibitors of Ser/Thr protein phosphatases: specificity, use and common forms of abuse. *Methods Mol Biol* **365:**23–38.
Swingle MR, Honkanen RE, and Ciszak EM (2004) Structural basis for the catalytic activity of human serine/threonine protein phosphatase-5. *J Biol Chem* **279:**33992–33999.
Trost BM, Frederiksen MU, Papillon JP, Harrington PE, Shin S, and Shireman BT (2005) Dinuclear asymmetric Zn aldol additions: formal asymmetric synthesis of fostriecin. *J Am Chem Soc* **127:**3666–3667.
Usui T, Marriott G, Inagaki M, Swarup G, and Osada H (1999) Protein phosphatase 2A inhibitors, phoslactomycins. Effects on the cytoskeleton in NIH/3T3 cells. *J Biochem* **125:**960–965.
Walsh AH, Cheng A, and Honkanen RE (1997) Fostriecin, an antitumor antibiotic with inhibitory activity against serine/threonine protein phosphatases types 1 (PP1) and 2A (PP2A), is highly selective for PP2A. *FEBS Lett* **416:**230–234.
Weiner SJ, Kollman PA, Case DA, Singh UH, Ghio C, Alagona G, Profeta S, and Weiner P (1984) A new force field for molecular mechanical simulation of nucleic acids and proteins. *J Am Chem Soc* **106:**765–784.
Xing Y, Xu Y, Chen Y, Jeffrey PD, Chao Y, Lin Z, Li Z, Strack S, Stock JB, and Shi Y (2006) Structure of protein phosphatase 2A core enzyme bound to tumor-inducing toxins. *Cell* **127:**341–353.
Zhang J, Zhang Z, Brew K, and Lee EY (1996) Mutational analysis of the catalytic subunit of muscle protein phosphatase-1. *Biochemistry* **35:**6276–6282.
Zhang Z, Zhao S, Long F, Zhang L, Bai G, Shima H, Nagao M, and Lee EY (1994) A mutant of protein phosphatase-1 that exhibits altered toxin sensitivity. *J Biol Chem* **269:**16997–17000.

**Address correspondence to:** Richard E. Honkanen, Department of Biochemistry and Molecular Biology, MSB 2362, 307 University Blvd. N., Mobile, AL 36688. E-mail rhonkanen@jaguar1.usouthal.edu